Solution Synthesis of Anisotropic Gold Microcrystals

Journal:	*ChemComm*
Manuscript ID	CC-COM-06-2020-004175.R1
Article Type:	Communication

COMMUNICATION

Solution Synthesis of Anisotropic Gold Microcrystals

Received 00th January 20xx,
Accepted 00th January 20xx

DOI: 10.1039/x0xx00000x

Bishnu P. Khanal and Eugene R. Zubarev

Wet chemistry methods have proven to be successful for the synthesis of nanocrystals. However, the size and shape control is often lost when dimentions of particles exceed several hundred nanometers. Therefore, a synthetic transformation of nano- to microcrystals in solution remains to be a challenge. Here we report a very efficient chemical synthesis of anisotropic microcrystals of gold and the set of experimental conditions that enables a precise control over their size and aspect ratio.

Last two decades have seen significant advances in the synthesis and potential applications of isotropic and anisotropic gold nanostructures.[1] Out of many synthetic approaches, the seed-mediated protocols with[2] and without[3] the use of silver nitrate are the most popular syntheses of single crystalline and pentahedrally-twinned gold nanorods, respectively. There have been several studies on the chemical synthesis and potential application of gold nanowires[4] and mesoscopic gold particles.[5] However, the preparation and physical properties of one-dimensional gold microstructures (referred to as gold mircorods (AuMRs)) have not been reported to date due to synthetic limitation. Here, we demonstrate a very efficient method for the solution synthesis of well-defined AuMRs by using pentahedrally-twinned gold nanorods (AuNRs) as seed particles. AuMRs were synthesized by the fast reduction of Au(I) to Au(0) on top of pre-synthesized AuNRs which resulted in the uniform amplification of AuNRs. It has been reported that the fast reduction of Au(I) to Au(0) on top of single crystalline gold nanorods resulted in the non-uniform deposition of Au(I) ions on the surface of nanorods which produced unwanted random shapes with complete loss of rod-like anisotropic morphology.[6] To our surprise, when pentahedrally twinned AuNRs were used as opposed to single crystalline AuNRs as seed particles, the very uniform deposition of Au(I) ions on the surface of pre-formed AuNRs with great retention in their pentahedral facets and rod shape was observed resulting in the formation of AuMRs. Most importantly, the length and width of AuMRs can be fully controlled by adjusting the amount of Au(I) ions introduced into the growth solution. In addition, the tip-selective deposition and dissolution technique[4a, 7] under reductive and oxidative conditions, respectively, can be successfully used to reversibly change the length of AuMRs while keeping their width constant, thus resulting in the formation of high and low aspect ratio AuMRs.

The pentahedrally-twinned AuNRs were synthesized by the method originally developed by Murphy *et al.*[3] This protocol produces the mixture of nanorods, platelets, and spherical particles. The purification and isolation of pure AuNRs was carried out by gravitational precipitation and partial dissolution technique.[8] Specifically, the mixture containing nanorods, platelets and spherical particles was kept undisturbed for 24 h to allow for the slow precipitation of nanorods and platelets while leaving lighter spherical particles and smaller nanorods in solution. The solution was carefully decanted, and the precipitate was dispersed in 0.1 M CTAB aqueous solution. Next, the mixture of AuNRs and platelets were treated with an oxidizing Au(III)/CTAB solution which partially dissolved AuNRs and platelets. The controlled dissolution followed by gravitational precipitation enabled the separation of heavier AuNRs as a precipitate and lighter disks/platelets as a decantation product. The isolated AuNRs were re-dispersed into 0.1 M CTAB solution and used as anisotropic seed particles for the growth of AuMRs.

For the AuMRs synthesis, the growth solution was prepared by dissolving $HAuCl_4 \cdot 3H_2O$, and CTAB in de-ionized water at 25 °C. Next, Au(III) ions were reduced to Au(I) by ascorbic acid (AA) which changed the color of growth solution from dark yellow to colorless. Pure AuNRs were used as seed and introduced into the growth solution upon vigorous stirring (~2-3 mins). The flask was hand-stirred every 2-3 hours to prevent the quick precipitation of partially grown AuMRs. Continuous stirring of solution was avoided because AuMRs precipitated prematurely and formed a golden-brown film at the inner wall of the flask.

---

[a] *Department of Chemistry, Rice University, 6100 Main Street, Houston, TX 77005, United States*

Electronic Supplementary Information (ESI) available: Experimental details, statistical size calculation, additional SEM images, UV-Vis-NIR spectra. See DOI: 10.1039/x0xx00000x

The initially used ratio of Au(I) ions to AuNRs seed was very high so we anticipated the formation of irregular morphologies due to fast deposition of Au(0) onto the surface of AuNRs. In contrast, we observed that even though the reduction proceeded at a high rate, Au(0) deposited uniformly onto the surface of AuNRs maintaining the initial morphology and crystal structure, while no unwanted shapes/impurities were generated. In fact, the Au(0) deposition was very even and smooth on all the crystal facets covering both the sides and the tips of the obtained structures. Careful analysis of several SEM images at high magnification did not show any defects and grain boundaries on the surface of AuMRs. The pentahedrally-twinned morphology of AuMRs could be very clearly seen in the SEM images of vertically standing microrods (Fig. SI 1). Fig. 1 shows the SEM images of AuMRs synthesized with different amounts of Au(I) added to the growth solution. The dimensions (length x width) of the resulting AuMRs were approximately 600 x 100, 800 x 160, 1000 x 200 and 1200 x 300 nm by using 12.5, 25, 50, and 100 µmol of Au(I), respectively. In all the cases, 500 µL of AuNRs seed solution was used. It was evident that the growth and the final size of AuMRs were proportional to the amount of Au(I) supplied in the growth solution. By varying the amount of Au(I) ions, the length and width of AuMRs can be controlled. When the concentration of Au(I) was low (12.5 and 25 µmol), smooth sides and tips were observed (Fig. 1 a,b). However, when the amount of Au(I) was higher (50 and 100 µmol), relatively thick AuMRs with low aspect ratio and pencil-like tips (Fig. 1 c,d) were observed because of the tip-preferential deposition of Au(0). Additionally, none of the starting AuNRs seeds were observed in SEM samples, which suggest that the amplification of AuNRs seed particles and the overall yield of AuMRs was nearly quantitative. Fig. SI 2 shows the low magnification SEM image of AuMRs, indicating that the purity of these structures is >98%.

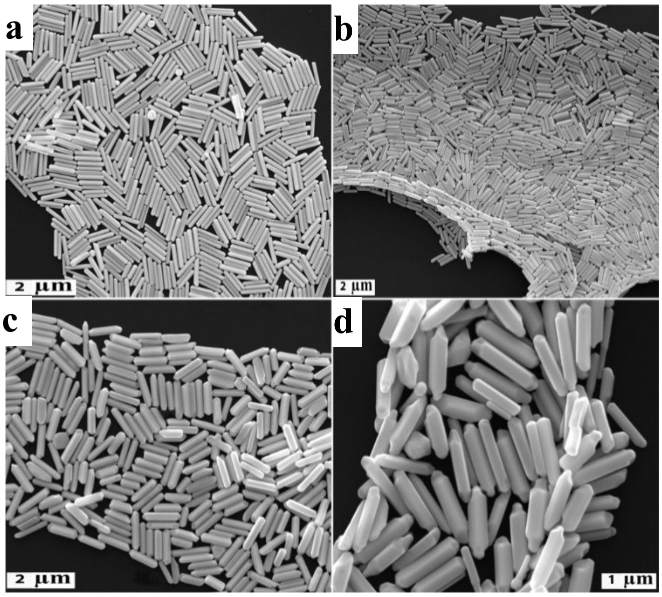

Figure 1. SEM images of AuMRs synthesized by fast deposition of Au (0) onto the AuNR seed particles. AuMRs of different dimensions (length x width): (a) 597.32 ± 101.47 nm x 108.26 ± 7.11 nm, (b) 796.43 ± 116.20 nm x 159.31 ± 10.13 nm, (c) 1028.50 ± 156.39 nm x 200.95 ± 14.68 nm and (d)1189.50 ±180.64 nm x 300.12 ± 20.22 nm.

Table 1. Length and width of AuMRs obtained with various amount of Au (I) ions in the growth solution.

Amount of Au(I) µmol	**Length (nm)**	**Width (nm)**	**Aspect ratio**
12.5	597.32 ± 101.47	108.26 ± 7.11	5.54 ± 1
25.01	796.43 ± 116.20	159.31 ± 10.13	5.09 ± 0.79
50.02	1028.50 ± 156.39	200.95 ± 14.68	5.15 ± 0.92
100.04	1189.50 ±180.64	300.12 ± 20.22	3.98 ± 0.67

Both the length and width of AuMRs increase with the increase in Au (I), however the size distribution becomes wider as seen by the increase in standard deviation. Not only the size distribution becomes wider, but also the aspect ratio decreases with the increase in Au (I) ions concentrations which suggests a faster and side-preferential deposition of Au (0).

The purity of the synthesized AuMRs was governed by the initial purity of AuNRs seed particles. We noticed that few platelets and spherical particles (<2 %) left as impurities during the purification of AuNRs seeds, also maintained their morphologies and grew to form bigger platelets and particles. Therefore, the uniform amplification process described here is not limited to AuNRs, and can be potentially applied to various other shapes. A separate experiment was conducted to induce the growth of nanoplatelets and spherical particles (not shown) by using them as seed particles. Interestingly, not only the spherical particles and 2D faceted platelets grew bigger in size, but also the sharp facets and starting morphology were very well maintained during the amplification process indicating the uniform deposition of Au(0) on the surface of platelets (Fig. SI 3).

Fig. 2 shows the histograms for size (length and width) and aspect ratio distribution of AuMRs. At low concentration of Au(I) ions in the growth solution, uniform growth with narrow size distribution was observed. However, when the amount of Au(I) was increased, not only the size distribution became broader as observed by significant increase in their standard deviation (σ = 101.47 for 597.32 nm and σ = 180.64 for 1189.50 nm AuMRs), but also the non-uniform pencil-like tips were observed. Figs. SI 4-7 show the detailed statistical data analysis for the size distribution.

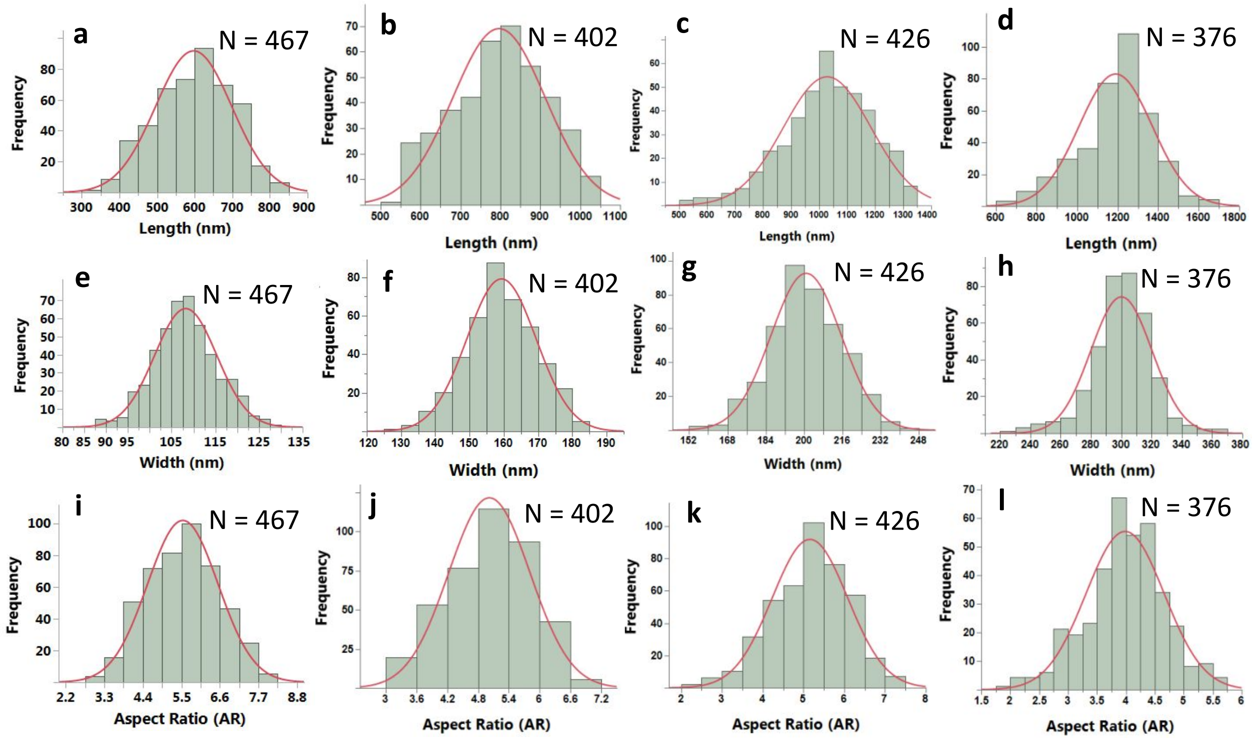

Figure 2. Histograms showing the AuMRs length a) 597.32 ± 101.47 nm, b) 796.43 ± 116.20 nm, c) 1028.50 ± 156.39 nm, and d) 1189.50 ±180.64 nm, width e) 108.26 ± 7.11 nm, f) 159.31 ± 10.13 nm, g) 200.95 ± 14.68 nm and h) 300.12 ± 20.22 nm, and their aspect ratio i) 5.54 ± 1.0, j) 5.0 ± 0.79, k) 5.15 ± 0.91 and l) 3.98 ± 0.67. N represents the sample size.

The increase in length and width of AuMRs were proportional to the amount of Au(I) used in the growth solution. The higher the amount of Au(I) in growth solution, the greater the length and width of the resulting AuMRs. Table 1 shows the final length and width of AuMRs obtained by using various amount of Au(I) in the growth solution. Both dimensions increased with the increase in the amount of Au(I) added, however the polydispersity of resulting AuMRs increased (as seen by the increase in standard deviation) at higher concentration of Au(I) ions (Fig. 2 and SI 4-7). The aspect ratio also decreased with the increase in Au(I) concentrations. The average increase in width was ~2.5 times higher than the increase in average length, which suggested that during fast deposition of Au(0) there was some preference for deposition on the sides versus the tips of AuMRs (Fig. SI 8). To demonstrate the actual visual differences on the size of starting seed AuNRs particles and the final AuMRs, an SEM sample was prepared by mixing AuNRs and AuMRs and examined under SEM. A dramatic difference in dimensions (Fig. SI 9) can be clearly seen in this case.

It has been previously reported that electrochemically-templated polycrystalline gold rods (85nm in diameter) exhibit higher-order multipole resonances when suspended in D_2O.[9] We expected to see similar higher-order multipole resonance given the large size of AuMRs synthesized in our study. Therefore, CTAB-stabilized water dispersible AuMRs of different sizes (~6000 nm x 300 nm, ~1200 nm x 300 nm, ~1000 nm x 200 nm, ~ 350 nm x 110 nm, ~450 nm x 200 nm) were examined by UV-Vis-NIR spectroscopy. However, we did not observe any appreciable signal from these gold microstructures (Fig. SI 10). None of the samples showed either longitudinal plasmon band (LPB) or higher-order multiple resonances except for a weak transverse plasmon peak at ~ 550 nm. The strong optical scattering due to higher volume of AuMRs might be the reason for the complete

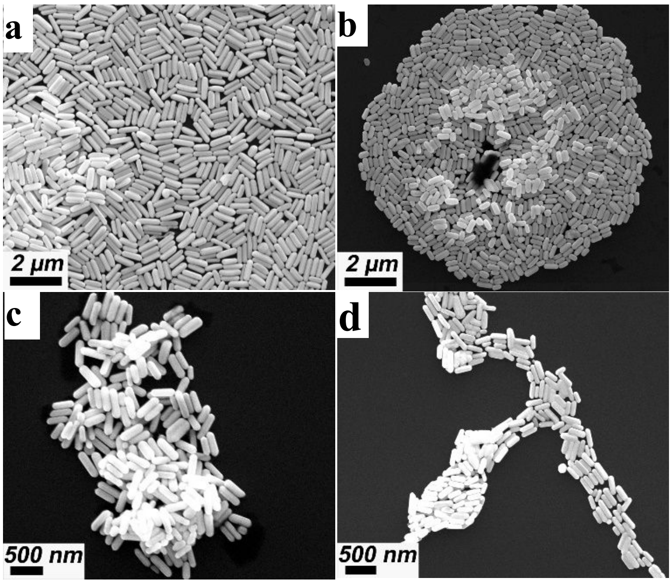

Figure 3. SEM images of ~800 nm x ~200 nm (a), ~450 nm x ~200 nm (b) and ~400 nm x ~110 nm (c), ~300 nm x ~110 nm (d) AuMRs obtained by the tip selective 1D dissolution of ~ 1028 nm x ~200 nm and ~600 nm x ~110 nm AuMRs, respectively. The SEM images clearly demonstrate the decrease in length of AuMRs while keeping their width constant during 1D dissolution process.

suppression of LPB. We believe, the strong optical scattering phenomenon and possible dephasing to new plasmon mode due to the larger size of AuMRs makes them perfect candidates for the study on their potential applications in surface enhanced Raman scattering (SERS), photocatalysis, photonics and bio-medical imaging.

Multiple possible growth mechanism has been discussed in literature for the growth of spherical gold nanoparticles to 1D AuNRs.[10] However, the detail mechanism on the transformation of small AuNRs to well-defined anisotropic microcrystal with uniform surface has to be yet determined. We believe that the growth process is reminiscent to the classical crystal growth process, therefore no localized deposition of Au to form unwanted morphology was observed. The deposition of gold atoms follows the original pattern of crystalline lattice during reduction of Au(I) ions to metallic gold on the surface of pre-formed AuNRs which can be confirmed by the clear visualization of pentahedral tips on the high magnification images of AuMRs (Fig. SI1).

Even though it was not possible to grow AuNRs one dimensionally under our experimental conditions, a post-synthesis size manipulation could be done on the resulting AuMRs to achieve the desired dimensions and aspect ratios. It has been previously reported that the tip-selective 1D growth and dissolution of gold nanorods was possible by using Au(I)/CTAB/AA and Au(III)/CTAB, respectively.[4a,7] Similar approach was taken for the length manipulation of AuMRs.

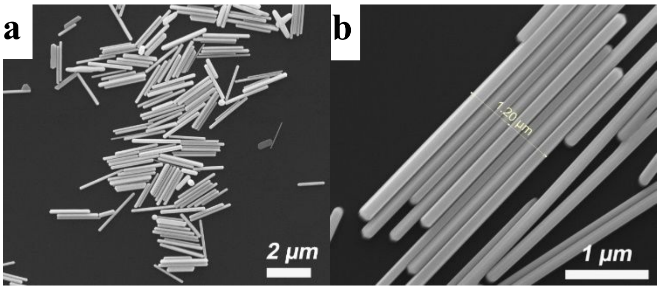

Figure 4. SEM images a) low magnification and b) high magnification of ~1.7 – 2 μm high aspect ratio AuMRs synthesized by one dimensional growth of AuMRs.

The 1D oxidative dissolution was carried out by treating AuMRs with Au(III)/CTAB complex. Dissolution of AuMRs with Au(III)/CTAB showed strong tips selectivity as observed in the case of AuNRs.[4a] However, the rate of dissolution was relatively slow because of their greater thickness and higher metallic gold content. Fig. 3 shows rod-like structures of various dimensions obtained by the dissolution of as-prepared AuMRs. Fig. 3 a,b shows the SEM images of 800 x 200 nm and 450 x 200 nm rods obtained by the dissolution of ~1028 x 200 nm AuMRs and Fig. 3 c,d presents the images of 400 x 100 nm and 300 x 100 nm rods obtained by the dissolution of 600 x 100 nm AuMRs. In strong contrast, the 1D growth of AuMRs to achieve high aspect ratio microstructures was carried out by using a tip-selective elongation technique in the presence of Au(I)/CTA/AA.[4a] The tip-selective growth of AuMRs resulted in the formation of high aspect ratio (~50) microrods. Fig. 4 and Fig. SI 11 show the images of the resulting high aspect ratio AuMRs. The dissolution and growth of AuMRs is fully reversible and can be stopped and resumed at any given point of reaction so that AuMRs of a desired length can be isolated from the solution.

Conclusions

In summary, we have demonstrated the first example of solution synthesis of gold microrods, whose length can be fully controlled and manipulated by changing the amount of Au(I) precursors in the growth solution. AuMRs of various dimensions were synthesized by varying the concentration of Au(I) ions in the reaction mixture. The growth process by using Au(I)/CTAB/AA as growth solution and gold nanostructures as seed, is not limited to AuNRs, but can also be applied to various other morphologies. The fine tuning of length of AuMRs was carried out by tip-selective dissolution and elongation technique with Au(III)/CTAB complex to synthesize shorter AuMRs and high aspect ratio AuMRs, respectively. The approach described here may offer a new opportunity for solution synthesis of other metallic and inorganic microcrystals.

This work was supported by NSF grant DMR-1105878.

Conflicts of interest

There are no conflicts to declare.

Notes and references

1. (a) J. Pérez-Juste, I. Pastoriza-Santos, L. M. Liz-Marzán and P. Mulvaney, *Coord. Chem. Rev.*, 2005, **249**, 1870-1901 (b) L. Vigderman, B. P. Khanal and E. R. Zubarev, *Adv. Mater.*, 2012, **24**, 4811-4841 (c) H. Chen, L. Shao, Q. Li and J. Wang, *Chem. Soc. Rev.*, 2013, **42**, 2679-2724 (d) D. P. Yang and D. X. Cui, *Chem. Asian J.*, 2008, **3**, 2010-2022 (e) M. Grzelczak, J. Pérez-Juste, P. Mulvaney and L. M. Liz-Marzán, *Chem. Soc. Rev.*, 2008, **37**, 1783-1791 (f) S. E. Lohse and C. J. Murphy, *Chem. Mater.*, 2013, **25**, 1250-1261 (g) X. Huang, S. Neretina and M. A. El-Sayed, *Adv. Mater.*, 2009, **21**, 4880-4910 (h) J. Stone, S. Jackson and D. Wright, *Wiley Interdiscip. Rev.: Nanomed. Nanobiotechnol.*, 2011, **3**, 100-109.

2. B. Nikoobakht and M. A. El-Sayed, *Chem. Mater.*, 2003, **15**, 1957-1962.

3. N. R. Jana, L. Gearheart and C. J. Murphy, *J. Phy. Chem. B*, 2001, **105**, 4065-4067.

4. (a) B. P. Khanal and E. R. Zubarev, *ACS nano*, 2019, **13**, 2370-2378 (b) C. Wang, Y. Hu, C. M. Lieber and S. Sun, *J. Am. Chem. Soc.*, 2008, **130**, 8902-8903 (c) F. Kim, K. Sohn, J. Wu and J. Huang, *J. Am. Chem. Soc.*, 2008, **130**, 14442-14443 (d) Y.-N. Wang, W.-T. Wei, C.-W. Yang and M. H. Huang, *Langmuir*, 2013, **29**, 10491-10497 (e) K. Critchley, B. P. Khanal, M. L. Gorzny, L. Vigderman, S. D. Evans, E. R. Zubarev and N. A. Kotov, *Adv. Mater.*, 2010, **22**, 2338-2342.

5. (a) H. Wang and N. J. Halas, *Adv. Mater.*, 2008, **20**, 820-825 (b) E. C. Dreaden, A. M. Alkilany, X. Huang, C. J. Murphy and M. A. El-Sayed, *Chem.l Soc. Rev.*, 2012, **41**, 2740-2779 (c) C. Ziegler and A. Eychmuller, *J. Phy. Chem. C*, 2011, **115**, 4502-4506 (d) E. Panfilova, A. Burov and B. Khlebtsov, *Colloid J.*, 2020, **82**, 27-35 (e) L. Vigderman and E. R. Zubarev, *Langmuir*, 2012, **28**, 9034-9040.

6. B. P. Khanal and E. R. Zubarev, *Chem. Eur. J.*, 2019, **25**, 1595-1600.

7. J. Rodríguez-Fernández, J. Pérez-Juste, P. Mulvaney and L. M. Liz-Marzán, *J. Phy. Chem. B*, 2005, **109**, 14257-14261.

8. B. P. Khanal and E. R. Zubarev, *J. Am. Chem. Soc.*, 2008, **130**, 12634-12635.

9. (a) E. K. Payne, K. L. Shuford, S. Park, G. C. Schatz and C. A. Mirkin, *The J. Phy. Chem. B*, 2006, **110**, 2150-2154 (b) J. E. Millstone, S. Park, K. L. Shuford, L. Qin, G. C. Schatz and C. A. Mirkin, *J. Am. Chem. Soc.*, 2005, **127**, 5312-5313.

10. (a) M. J. Walsh, W. Tong, H. Katz-Boon, P. Mulvaney, J. Etheridge and A. M. Funston, *Acc. Chem. Res.*, 2017, **50**, 2925-2935 (b) S. K. Meena and M. Sulpizi, *Langmuir*, 2013, **29**, 14954-14961 (c) J. A. da Silva, P. A. Netz and M. R. Meneghetti, *Langmuir*, 2019, **36**, 257-263.

TOC Figure:

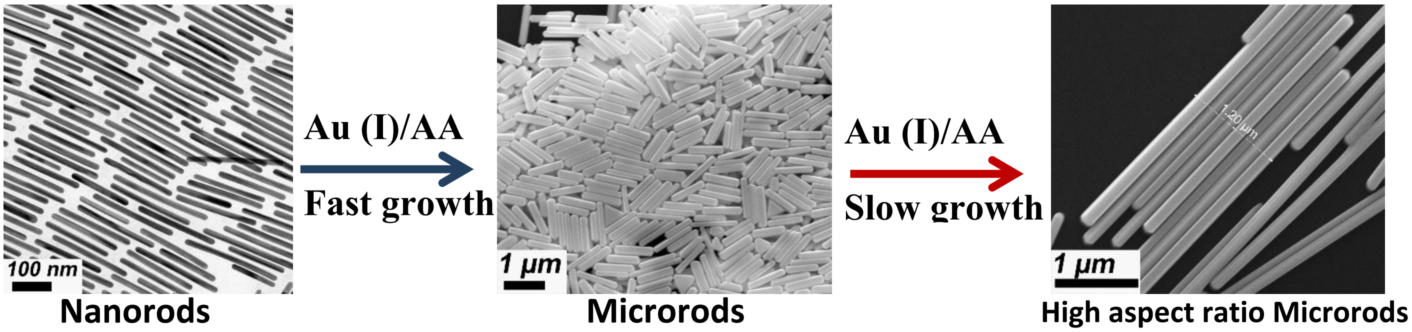

Amplification of pentahedrally twinned gold nanorods with Au(I)/AA results in the formation of very well-defined anisotropic microcrystals of gold referred as gold microrods.